Arabian Journal of Chemistry (2015) xxx, xxx–xxx

King Saud University

Arabian Journal of Chemistry

www.ksu.edu.sa
www.sciencedirect.com

ORIGINAL ARTICLE

Biogenic synthesis, characterization of antibacterial silver nanoparticles and its cell cytotoxicity

V. Gopinath [a,b,*], S. Priyadarshini [b], Mun Fai Loke [b], J. Arunkumar [c], Enrico Marsili [d], D. MubarakAli [e,f], P. Velusamy [a], Jamuna Vadivelu [b]

[a] Department of Biotechnology, School of Bioengineering, SRM University, Kattankulathur, Chennai 603 203, Tamil Nadu, India
[b] Department of Medical Microbiology, Faculty of Medicine, University of Malaya, 50603 Kuala Lumpur, Malaysia
[c] Department of Microbiology, SRM University, Sonepat, Haryana 131029, India
[d] Singapore Centre for Environmental Life Sciences Engineering (SCELSE), Nanyang Technological University, 637551, Singapore
[e] Division of Bioengineering, Incheon National University, Incheon, Republic of Korea
[f] Centre for Surface Technology and Applications, Korea Aerospace University, Republic of Korea

Received 10 August 2015; accepted 16 November 2015

KEYWORDS

Biosynthesis;
Pseudomonas putida;
Antimicrobial activity;
Cytotoxicity;
Biocompatibility;
Silver nanoparticles

Abstract The advanced research and development of silver nanoparticles (AgNPs) is vast due to their incredible applications today. In this work, AgNPs were synthesized using soil derived *Pseudomonas putida* MVP2. The AgNPs formation on the *P. putida* cell membrane and its cell free supernatant was studied. The synthesized AgNPs were characterized by UV–visible spectroscopy, scanning transmission electron microscopy (STEM), X-ray diffraction (XRD), energy dispersive X-ray (EDAX) and Fourier transform infrared (FTIR) spectrum analysis. The mode of action of AgNPs on the bacteria was studied against clinically isolated bacterial pathogens, *Staphylococcus aureus*, *Escherichia coli*, *Bacillus cereus*, *Pseudomonas aeruginosa* and *Helicobacter pylori* by membrane integrity, and protein leakage using confocal and electron microscopy. Interestingly, AgNPs had no cytotoxicity under 25 μg/mL and it was toxic at above 50 μg/mL on human epidermoid larynx carcinoma (HEp-2) cells. This study evidenced that biogenic nanoparticles could affect the bacterial replication, protein leakage and eventually cell death. This might be used for active antimicrobial agents for the chronic infections.
© 2015 The Authors. Production and hosting by Elsevier B.V. on behalf of King Saud University. This is an open access article under the CC BY-NC-ND license (http://creativecommons.org/licenses/by-nc-nd/4.0/).

1. Introduction

Conventional methods for metal nanoparticle synthesis normally require the use of highly toxic chemicals, solvents, capping agents and also extreme controlled conditions that increase cost and cause environmental pollution (Gopinath et al., 2012). The biogenesis of nanoparticles by a green chemistry approach could reduce the cost and would be eco-friendly in nature. For effective silver nanoparticles

* Corresponding author at: Department of Medical Microbiology, Faculty of Medicine, University of Malaya, 50603 Kuala Lumpur, Malaysia.
E-mail address: yele.gopi@gmail.com (V. Gopinath).
Peer review under responsibility of King Saud University.

Production and hosting by Elsevier

http://dx.doi.org/10.1016/j.arabjc.2015.11.011
1878-5352 © 2015 The Authors. Production and hosting by Elsevier B.V. on behalf of King Saud University.
This is an open access article under the CC BY-NC-ND license (http://creativecommons.org/licenses/by-nc-nd/4.0/).

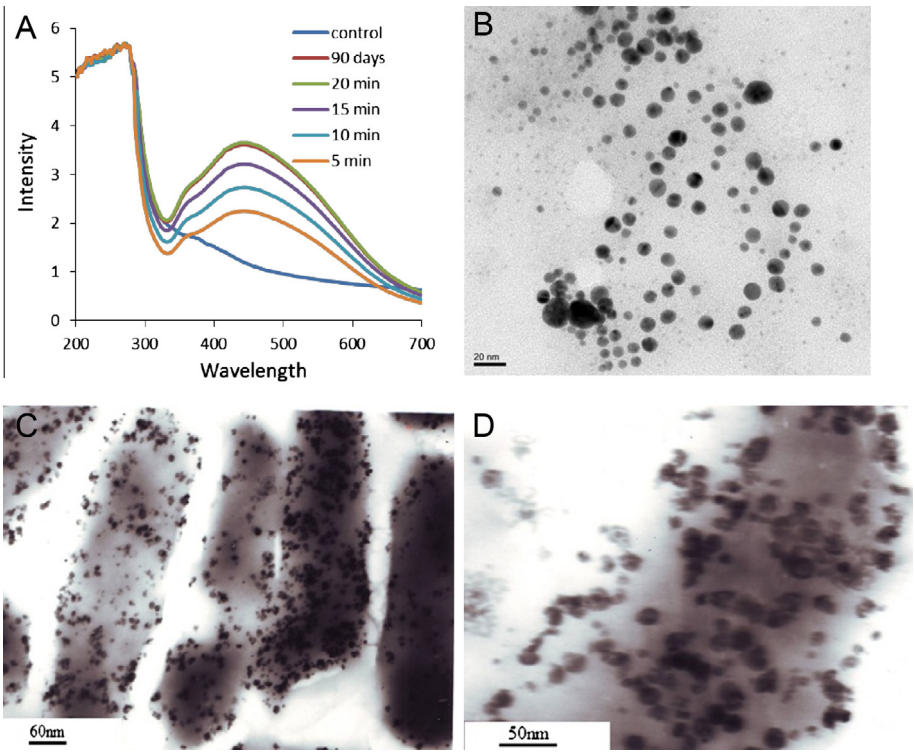

Figure 1 UV–Vis spectra of AgNPs synthesized using cell-free supernatant at increasing time for 0–20 min and 90 days at 37 °C (A), HRTEM images of AgNPs using cell free supernatant showed in the size ranges of 5–16 nm (B). TEM images of AgNPs synthesized using cell membrane (C and D).

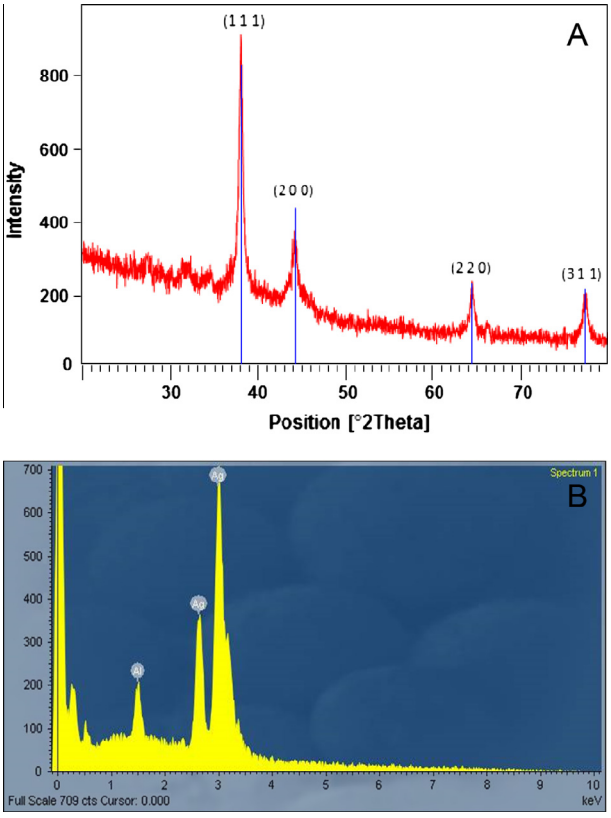

Figure 2 X-ray diffraction spectrum of biogenic AgNPs (A), EDAX spectrum showed elemental signals of silver (B).

(AgNPs) biosynthesis, *Bacillus flexus* was used as the reducing and stabilizing agent (Priyadarshini et al., 2013). Most of the biological aetiology has been used to generate metal nanoparticles (MubarakAli et al., 2011, 2013; Gopinath et al., 2013; Gajbhiye et al., 2009; Xie et al., 2007). On the other hand, the kinetics of the biosynthesis is much faster when cell-free extracts were used (Tamboli and Lee, 2013; Kalpana and Lee, 2013). Recently electrochemically active biofilm mediated silver nanocomposite has been synthesized with higher antibacterial and photocatalytic activity (Ansari et al., 2014; Khan et al., 2013, 2014).

The AgNPs are superior disinfectants that can significantly reduce many bacterial infections for longer period compared to usage of common biocides, penicillin, and tetracycline. AgNPs are very effective since they are potent biocides against various microorganisms such as bacteria, fungi, and viruses. Certain bacteria are resistant to antibiotics, and some have developed resistance. For examples, *Neisseria gonorrhoeae*, *Staphylococcus aureus* and *Helicobacter pylori* are resistant to penicillin and metronidazole (Teh et al., 2014; Madhavan et al., 2014). *H. pylori* infection is considered to be a primary risk factor for the development of gastric ulcer and gastric cancer. However, *H. pylori* resistance to most of the commonly used antibiotics is increasing worldwide and alternate approaches have been proposed to overcome the side-effects associated with antibiotic treatment for *H. pylori* (Iwanczak and Iwanczak, 2012; Chang et al., 2011). It has been proposed that the antibacterial activity is based on the electrostatic attraction between negative charged cell membrane of microorganism and positive charged Ag ion. Therefore, Ag^{+} can cause bacterial cell death by damaging the cell membrane, strongly interacts with thiol groups of vital enzymes and destroying DNA replication ability (Shao et al., 2015).

Metallic Ag ions are inert but when it becomes ionized, it is highly reactive in water. Ionized silver causes structural changes to the bacterial cell wall and nuclear membrane, leading to cell distortion and death (Rai et al., 2009). In this study, we report on the extracellular

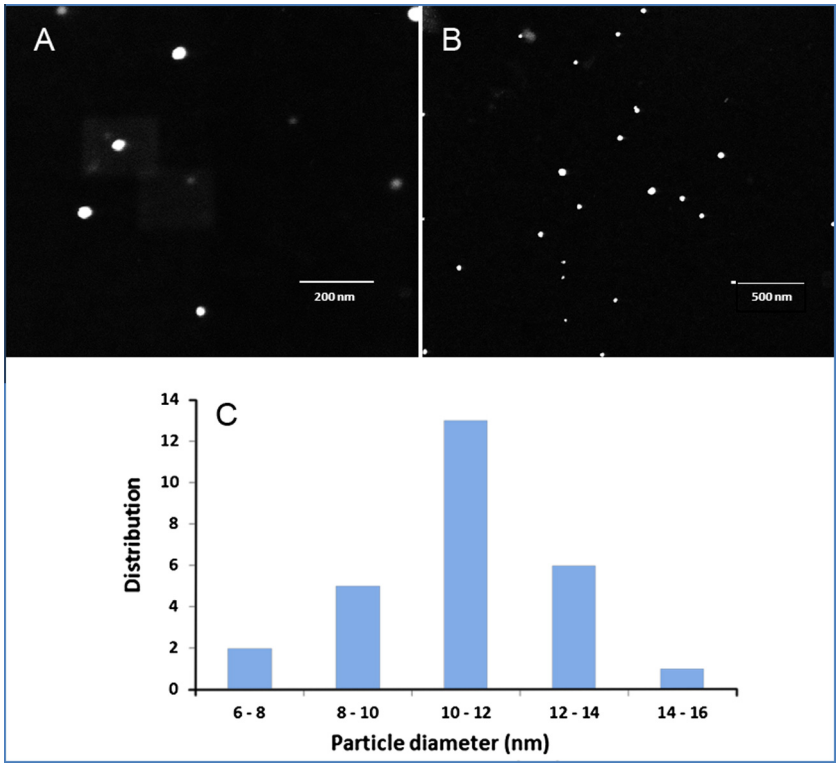

Figure 3 STEM images of AgNPs: monodispersed, spherical AgNPs with the size range from 6 to 16 nm (A and B); size distribution of AgNPs (C).

synthesis of AgNPs using *Pseudomonas putida* MVP2 derived from soil. The biosynthesized AgNPs exhibited considerable antibacterial activity against clinically isolated bacterial pathogens, *S. aureus*, *Pseudomonas aeruginosa*, *Escherichia coli* and *Bacillus cereus* and *H. pylori* strains (J99, NCTC 11637 and UM066).

2. Materials and methods

2.1. Chemicals

Analytical grade Silver nitrate ($AgNO_3$) was purchased from Sigma Aldrich (St. Louis, USA). The media components Mueller Hinton agar and Luria-Bertani agar were purchased from Himedia Laboratories, Mumbai, India, and Blood Agar media was purchased from Oxoid, UK.

2.2. Bacterial pathogens and cancer cell line maintenance

The bacterial clinical isolates *S. aureus*, *E. coli*, *B. cereus* and *P. aeruginosa* were obtained from SRM University Hospital, Tamil Nadu, India. The clinical isolate *H. pylori* UM066 was obtained from the Helicobacter Research laboratory, University of Malaya, Kuala Lumpur, Malaysia. *H. pylori* J99 (ATCC 700824) and NCTC 11637 (ATCC 43504) were obtained from American Type Culture Collection (ATCC, USA). The human epidermoid larynx carcinoma cell line (HEp-2) was obtained from the National Centre for Cell Sciences (NCCS), Pune, India. The HEp-2 cell lines were cultured in 25 cm^2 of a tissue culture flask with Minimum Essential Medium Eagle (MEM) supplemented with 10% foetal bovine serum (FBS), Earle's salts, L-glutamine, sodium bicarbonate, and antibiotic solution containing penicillin (100 μg/mL), streptomycin (100 μg/mL), kanamycin (50 μg/mL), and amphotericin B (25 μg/mL). The cultured cell lines were incubated at 37 °C in a humidified incubator containing 5% CO_2 (RS Biotech, UK).

2.3. Isolation, screening and identification of an efficient bacterial strain for AgNPs

The soil samples were collected from the waste dump sites of silver mining areas in Salem, Tamil Nadu, India. The serially diluted soil samples were plated on Luria–Bertani (LB) agar media and incubated at 37 °C for 24 h. After the incubation period, the bacterial colonies were observed and subcultured further in the same medium to obtain pure colonies. In a pilot scale screening, a total of 73 bacterial strains were isolated and named MPV1 to MPV73. All the isolates were freshly inoculated in LB broth and kept in a rotary shaker incubator for 37 °C at 160 rpm. The culture was then centrifuged at 8000 rpm and the supernatant was mixed with $AgNO_3$ to adjust the final volume concentration to 1 mM. Based on the rapid reduction of metallic silver (Ag^+) ions, one effective synthesizer was selected and identified as *P. putida* by *16S rRNA* sequencing. This isolate was named *P. putida* MPV2 (Priyadarshini et al., 2013).

2.4. Extracellular synthesis of AgNPs

The 24 h grown fresh culture of *P. putida* MPV2 in the LB broth was centrifuged at 8000 RPM for 10 min to obtain the supernatant. The supernatant was mixed with $AgNO_3$ solution

Table 1 Antibacterial activity of synthesized silver nanoparticles: diameter of zone of inhibition against *P. aeruginosa*, *E. coli*, *S. aureus*, *B. cereus*, *H. pylori* J99, *H. pylori* NCTC 11637 and *H. pylori* UM66.

SI. no. bacteria	Parameters	
	Concentration of AgNPs (μg/ml)	Zone of inhibition (mm)
		Mean of three replicates
1. *P. aeruginosa*	5	7.5
	10	8.6
	15	10.5
	20	12.2
2. *E. coli*	5	6.8
	10	7.7
	15	10.2
	20	12.1
3. *S. aureus*	5	6.7
	10	7.4
	15	8.9
	20	11.2
4. *B. cereus*	5	6.5
	10	7.8
	15	9.8
	20	11
5. *H. pylori* J99	5	0
	10	6.7
	15	7.5
	20	8.8
6. *H. pylori* NCTC 11637	5	0
	10	0
	15	6.8
	20	8.2
7. *H. pylori* UM66	5	0
	10	6.9
	15	7.2
	20	8.4

to make a final volume concentration of 1 mM. The supernatant without addition of $AgNO_3$ was maintained as a control. In another set of experiments the 24 h grown culture of *P. putida* was directly mixed with $AgNO_3$ to adjust the final concentration of 1 mM. The bacterial culture without addition of $AgNO_3$ was maintained as a control. Subsequently, the bioreduction of silver ions was monitored by the visual colour change and UV–visible spectrum analysis of the reaction mixture.

2.5. Physical characterization of the synthesized AgNPs

The UV–Vis spectrum analysis was recorded for the $AgNO_3$–bacteria reaction mixture by Perkin–Elmer double beam spectrophotometer (Lambda 45, Perkin–Elmer, USA). The samples were scanned in the range of 200–700 nm at a resolution of 1 nm. The functional association of the AgNPs was analysed by FTIR spectrum (Cary 660, Agilent technologies, USA) by the samples mixed with KBr to make a pellet and

Table 2 MIC values of synthesized AgNPs against tested bacterial strains.

SI. no. bacteria	Parameters	
	MIC (μg/ml)	MBC (μg/ml)
1. *P. aeruginosa*	7.5	9
2. *E. coli*	6.75	8
3. *S. aureus*	9	12.5
4. *B. cereus*	10.25	14
5. *H. pylori* J99	15	18.5
6. *H. pylori* NCTC 11673	25	25
7. *H. pylori* UM66	14.5	18

the spectrum was recorded at a resolution of 4 cm^{-1} at the range of 500–4000 cm^{-1}. The crystalline nature of the synthesized nanoparticles was characterized by X'Pert Pro A Analytical X-ray diffractometer instrument operated at 40 keV with Cu Kα radiation in a θ–2θ configuration. The topographical image of the nanoparticles was recorded by STEM. The sample was prepared by loading a drop of the nanoparticles solution on a carbon-coated copper grid followed by air-drying for 30 min.

2.6. Antibacterial investigation of biogenic AgNPs

2.6.1. Disc diffusion assay

Antibacterial activity of the biosynthesized AgNPs was evaluated by standard disc diffusion method according to National Committee for Clinical Laboratory Standards (NCCLS). About 10^4 colony forming units (CFUs) of bacterial cells such as *S. aureus*, *E. coli*, *P. aeruginosa* and *B. cereus* were spread on Mueller Hinton Agar (MHA) plates to create a confluent lawn of bacterial growth. The paper disc at 6 mm dimension was impregnated with different concentrations of AgNPs (5, 10, 15 and 20 μg/mL). The plates were incubated at 37 °C for 24 h and the diameter of the clear zone of inhibition around the disc was measured in mm. To test antibacterial activity for *H. pylori* strains of J99, NCTC 11637 and UM066, 72 h grown culture (about 10^4 CFUs) was inoculated in chocolate blood agar media supplemented with 7% of lysed horse blood. The plates were incubated at 37 °C for 72 h under microaerophilic conditions and the diameter of the clear ZOI around the disc was measured in mm and the triplicate mean value was calculated.

2.6.2. Determination of the minimum inhibitory concentration (MIC)

MIC of AgNPs was determined according to Clinical and Laboratory Standards Institute (CLSI) by the broth microdilution method (Mohan et al., 2014). The test pathogens were subcultured and then adjusted to 0.5 M McFarland standard to give $\sim 10^8$ CFU/mL. A 50 μL aliquot of the bacterial suspension was dispersed in 96-well plate containing various concentrations of AgNPs (2.5–50 μg/mL) resulting in 5×10^5 CFU/mL. Microtitre plate wells containing the MHB served as a negative control and the wells containing bacterial suspension served as a positive control. To determine the MIC of AgNPs against *H. pylori* strains J99, UM066 and NCTC 11637 bacteria were grown freshly for 72 h on brain heart infusion medium

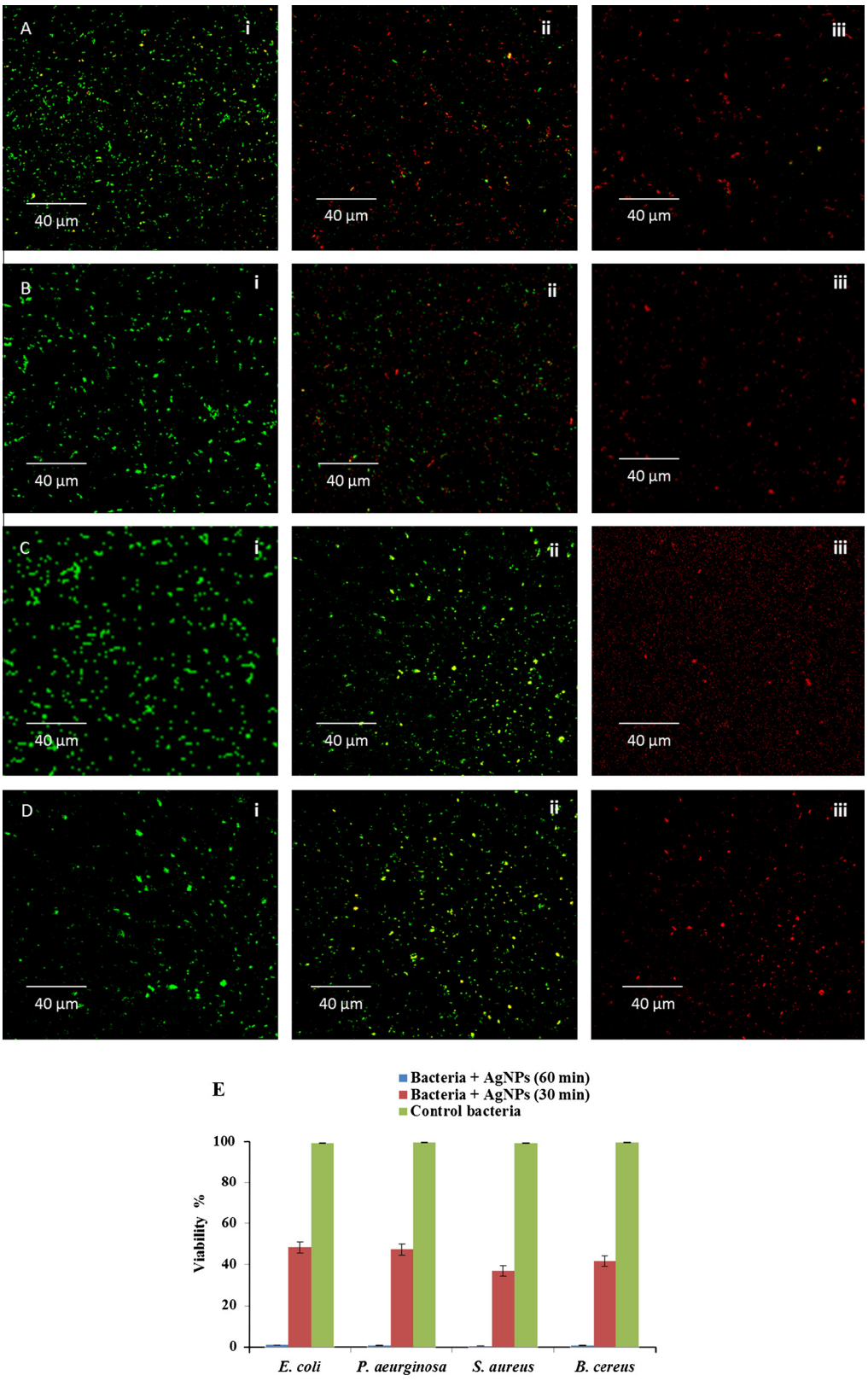

Figure 4 Live/dead cell staining confocal images of control bacterial cells *P. aeruginosa* (A i), *E. coli* (B i), *S. aureus* (C i) and *B. cereus* (D i); images (ii) and (iii) were AgNPs treated bacteria after 30 and 60 min of incubation respectively for *P. aeruginosa*, *E. coli*, *S. aureus* and *B. cereus*. (E). Viability percentage histogram of bacterial cells after nanoparticles treatment.

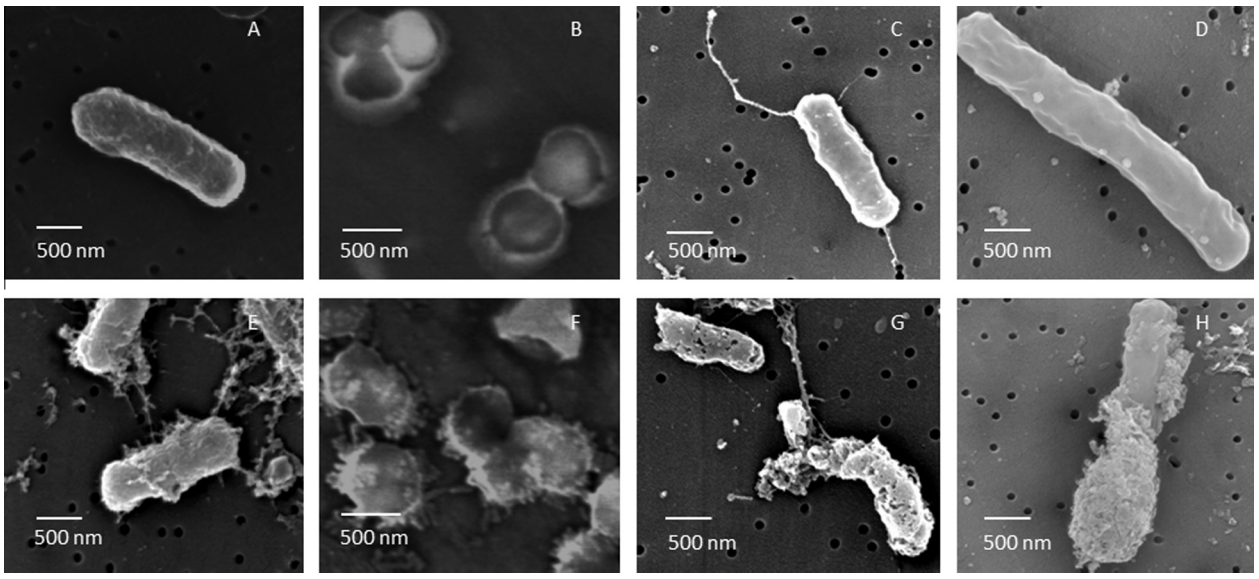

Figure 5 FE-SEM study of bacteria treated and untreated with AgNPs: morphology of *B. cereus*, *S. aureus*, *E. coli* and *P. aeruginosa* (A–D); bacterial cells treated with AgNPs showed membrane damage after 60 min of treatment (E–H).

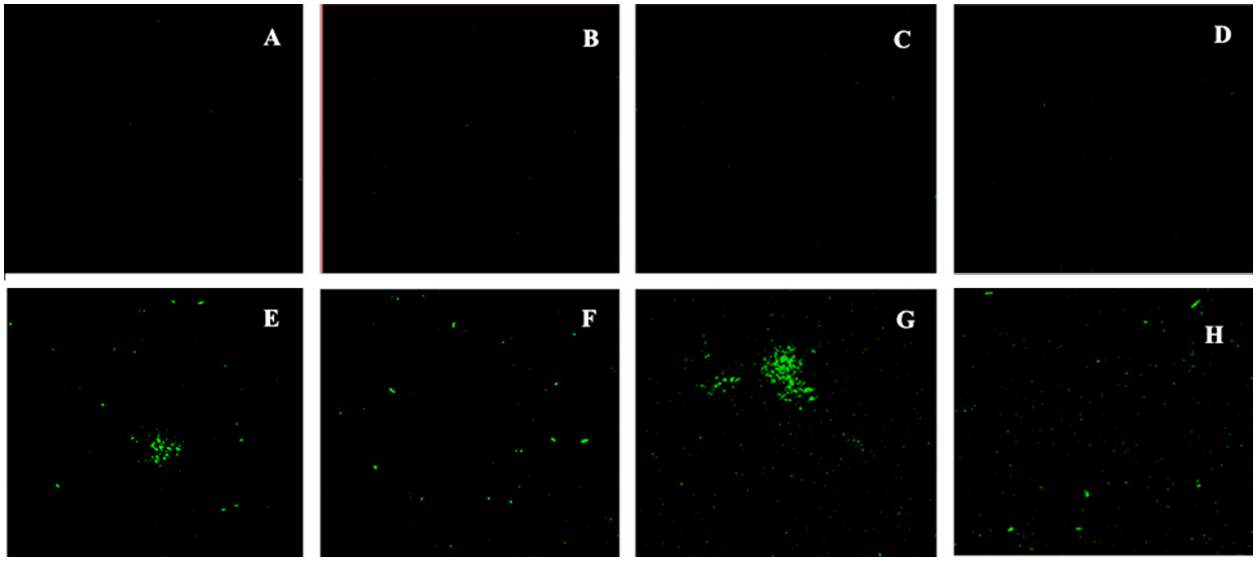

Figure 6 Bacterial intracellular protein leakage study showing green fluorescence confirmed protein leakage from the bacterial cells, *E. coli*, *P. aeruginosa*, *S. aureus*, *B. cereus* (E–H); untreated cells showing no fluorescence (A–D).

(BHI). The concentrations of the cultures were adjusted using BHI medium to give $\sim 10^8$ CFU/mL. MIC and minimum bactericidal concentration (MBC) were determined based on the bacterial growth.

2.6.3. Assessment of bacterial cell membrane damage

The ultrastructural changes in bacterial morphology caused by AgNPs were examined by field emission scanning electron microscopy (FESEM). The appropriate growth conditioned bacterial suspension was mixed with AgNPs and incubated for 30 min at 37 °C. The bacterial cells were then centrifuged at 6000 rpm for 10 min at 4 °C. The pellets obtained were washed twice with PBS at pH 7 before the samples were fixed with 8% glutaraldehyde (1:1 v/v) and Sorensen's phosphate buffer (SPB) for 60 min. 1:1 (v/v) of SPB and water mixture was applied before the samples were fixed with 4% Osmium tetroxide (OsO_4) mixed with 1:1 (v/v) H_2O. After overnight incubation, samples were washed with deionized water for 15 min and then dehydrated in increasing concentrations of ethanol. Dehydration with ethanol–acetone mixture followed by pure acetone was applied before critical point drying (CPD). The samples were then assessed under FESEM (JEOL JSM-7001F, Germany) to visualize the morphological changes of bacterial cells before and after AgNPs treatment.

2.6.4. Live/dead bacterial (backlight) assay

Live and dead bacterial cells assessment was studied with Live/Dead Backlight L-7012 (Invitrogen, SA, Spain) using confocal laser scanning microscopy (CLSM). The overnight grown test bacterial strains were adjusted to the concentration of

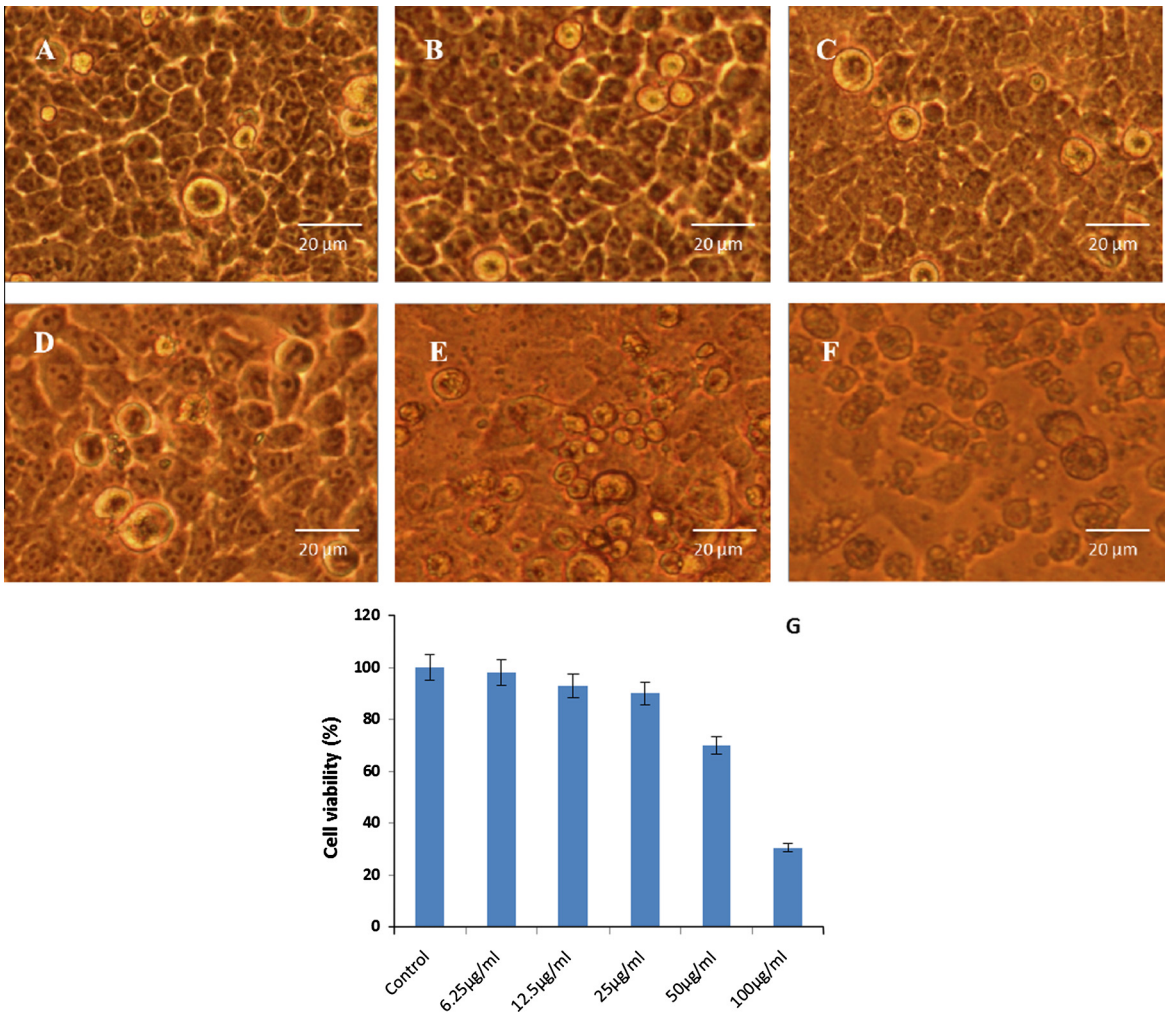

Figure 7 *In vitro* cytotoxicity effect of synthesized AgNPs on HEp-2 cell lines. (A) Showing healthy control cells; non-toxicity observed from concentrations of 6.25, 12.5, 25 µg/mL of AgNPs treatment (B–D); LD_{50} of AgNPs was determined at 50 or 100 µg/mL (E and F). The cell viability percentage of AgNPs at various concentrations of AgNPs (G).

$\sim 10^5$ CFU/mL. The bacterial cells were treated with the MBC concentrations of AgNPs and treated for 30 and 60 min. The cells were then collected by centrifugation at 6000 rpm for 5 min at 4 °C. The obtained pellet was washed with PBS following which the cells were stained with SYTO 9 and propidium iodide (PI) for 15 min under dark conditions. The stained bacterial cells were observed under CLSM (Carl Zeiss; 710-META, USA) to record fluorescent images. The fluorophores were excited using an Argon laser at 488 nm and a HeNe laser at 543 nm (Cai et al., 2011).

2.6.5. Leakage of intracellular molecules

The intracellular leakage of molecules from the AgNPs treated bacteria was studied using the fluorescent dye, FITC-I. The AgNPs-treated four bacterial strains were centrifuged at 8000 rpm for 6 min at 4 °C. The supernatant was then mixed with FITC-I (a green fluorescent dye) for 30 min at 37 °C under dark conditions. Then 25 µL samples were placed on a glass slide for CLSM imaging (Carl Zeiss; 710-META, USA).

2.7. In vitro evaluation of biocompatibility of biogenic AgNPs

The cell viability of HEp-2 cells was evaluated using nanoparticles by MTT assay (MubarakAli et al., 2015a,b). The 100 µL cell suspension was seeded in a 96-well tissue culture plate (5×10^4 cells/well) and incubated at 37 °C in a humidified 5% CO_2 incubator. After 24 h the growth medium was removed. The freshly prepared AgNPs in 5% DMEM were serially diluted eight times by a two-fold dilution (100–0.8 µg/mL) and each concentration of 100 µL was added in triplicate to the respective wells and incubated at 37 °C in a humidified 5% CO_2 incubator. After 72 h, the plate was observed for any changes in morphology and cell density by inverted phase contrast microscopy (Nikon, Japan). The content of the wells was then removed and 10 µL of the reconstituted MTT solution was added to all the test and control wells. The plate was gently shaken and incubated at 37 °C in a humidified 5% CO_2 incubator for 4 h, following which the supernatant was removed and 100 µL of a MTT solubilization solution (10% Triton X-100) in acidic isopropanol (0.1 N

HCL) was added to the formazan crystals. The absorbance was measured using a microplate reader at a wavelength of 570 nm.

3. Results and discussion

3.1. Biosynthesis of AgNPs in viable culture and cell free supernatant

Total of 73 bacterial strains were isolated and named MPV1 to MPV73. The cultures were then centrifuged at 8000 rpm and the supernatant was mixed with $AgNO_3$ to adjust the final volume concentration to 1 mM. Based on the rapid reduction of silver (Ag^+) ions, one effective synthesizer was selected and found to be MPV2 (data not shown). The strains were identified as *P. putida* by 16S rRNA sequencing. The colour change of the reaction mixture was observed from its original pale yellow to dark brown which primarily indicates the formation of AgNPs (Mukherjee et al., 2009). In parallel, *P. putida* broth culture was treated with $AgNO_3$ after 20 min incubation observed the colour change of dark brown from its original state. It may be because the bacterial cell membrane protein reduced the Ag^+ to Ag^0. HRTEM image revealed that the formation of AgNPs in the cell free supernatant (Fig. 1B) and TEM images revealed the formation of AgNPs on the cell membrane (Fig. 1C and D). Various magnification of $AgNO_3$ treated bacteria showing number of black spots on the bacterial membrane and cytoplasm. These results strongly proved that AgNPs were mostly synthesized in the outer membrane of the bacteria. The obtained results corroborate with the earlier report of extracellular production of AgNPs on *Verticilium* sp. and *Chlamydomonas reinhardtii* (Barwal et al., 2011; Sastry et al., 2003). Based on this study, further investigation was performed only with AgNPs prepared by cell free supernatant.

3.2. Physical characterization of biogenic AgNPs

The preliminary AgNPs synthesis reaction was monitored by UV–Vis spectra scanning of the cell-free extract which had been introduced with $AgNO_3$. After 20 min of incubation the reaction mixture showed a broad spectrum of peak at 420 nm which is the characteristic of AgNPs (Fig. 1A). The peak intensities increased at 5–20 min, which indicates growth as well as the formation of AgNPs in the reaction mixture. In the control sample of cell-free extract the peak was observed at 280 nm, which is characteristic of the biomolecules (Gopinath and Velusamy, 2013). Interestingly there is no precipitation observed for synthesized AgNPs solution over 90 days of storage at 37 °C and the sample was scanned at the same wavelength. The resultant spectrum showed no considerable change in the peak position compared with earlier observation of SPR peak at 420 nm, which indicated the biogenic AgNPs were highly stable after three months (Muniyappan and Nagarajan, 2014).

The FTIR spectrum of the cell-free extract alone showed five distinct peaks at the range of 3695, 3496, 1451, 1292, and 1166 cm^{-1} (Fig. S1). The band at 3695, 3496 cm^{-1} was referred as the strong stretching vibrations of the OH– functional group (Gopinath et al., 2012). The peak at 1451 cm^{-1} was due to the symmetric stretching vibrations of the COO– functional group (Sanghi and Verma, 2009), and 1292 cm^{-1} was assigned to the amide functional groups present in the cell free supernatant (Shivshankar et al., 2003). The band at 1166 cm^{-1} was attributed to the C–O– stretching vibrations (Angajala et al., 2014). The FTIR spectrum of biogenic AgNPs showed five peaks in the range of 3701, 3496, 1444, 1306 1181 and 1134 cm^{-1}. To compare the IR spectrum of the cell free supernatant and synthesized AgNPs, the major shifts were observed in the hydroxyl and carboxyl functional groups of protein which may be responsible for AgNPs synthesis.

The crystalline structure of biogenic AgNPs was confirmed by XRD. The diffraction spectrum of AgNPs showed face centred cubic (FCC) crystalline nature of four intense peaks (Fig. 2A) at 38.95°, 45.12°, 65.39° and 78.12° 2θ corresponding to plane values of (1 1 1), (2 0 0), (2 2 0) and (3 1 1) which were consistent with the standard data JCPDS file no. 01-087-0717 (Khan et al., 2012). The chemical composition of biogenic AgNPs was obtained from EDAX spectrum analysis (Fig. 2B). The resultant spectrum was observed with high intensity signals of Ag which indicated the presence of AgNPs. The signal showed at the Al peak which was used to load AgNPs sample for analysis.

STEM images showed the biogenic AgNPs obtained from the culture supernatant of *P. putida* were monodispersed, spherical shaped AgNPs with the size ranging from 6 to 16 nm. The nanoparticles images obtained in the different magnification ranges for the nanoparticle surface are shown (Fig. 3A and B). The average size distribution histogram of synthesized AgNPs is shown in Fig. 3C.

3.3. Antibacterial efficacy of biogenic AgNPs

3.3.1. Agar disc diffusion assay

In vitro antibacterial activity of biogenic AgNPs was determined by agar disc diffusion assay. The clear zone of inhibitions (ZOI) was observed around discs loaded with AgNPs, which clearly indicates that biogenic AgNPs showed a strong antimicrobial effect (Fig. S2). The mean diameters of the ZOI for the biogenic AgNPs were measured and tabulated (Table 1). No ZOI was observed for the control disc. The most possible antibacterial mechanism is due to Ag^+ released from AgNPs, which strongly binds to thiol groups found in enzymes and proteins on the cellular surface and can interfere with cell division and lead to bacterial cell death (Faria et al., 2014). Moreover, AgNPs can cause oxidative damage by producing reactive oxygen species (ROS), leading to attack enzymes and proteins resulting in irreversible damage to DNA replication (Markowska et al., 2013; MubarakAli et al., 2015a,b). The present study clearly indicates antibacterial activity of AgNPs against both Gram positive and Gram negative bacteria. Interestingly the biogenic AgNPs showed a considerable inhibitory pattern against *H. pylori* J99, *H. pylori* UM066 and *H. pylori* NCTC 11637 under appropriate conditions (Pathak et al., 2014). Comparatively, the *H. pylori* NCTC 11637 strain was considered not effective, when the concentration was higher than any other bacteria used in this study.

3.3.2. Minimum inhibitory concentration of AgNPs

To obtain the MIC values of biogenic AgNPs the broth culture of *E. coli*, *P. aeruginosa*, *S. aureus* and *B. cereus* was used. From the observed results AgNPs showed stronger bacterial growth inhibitory activity towards the Gram negative bacterial

strains of *P. aeruginosa* and *E. coli* (MIC 6.25 and 7 μg/mL) which is lower than the Gram positive strains of *B. cereus* and *S. aureus* (MIC 9 and 8.5 μg/mL) respectively. The absorbance (λmax_{600}) decreased along with the increasing concentration of nanoparticles for all the bacterial strains (Yang et al., 2014). The average of three replicate values of AgNPs against the tested strains is listed in Table 2. Recently Tamboli et al., (2013) reported that biosynthesis of AgNPs using bacterial isolate *Exiguobacterium* sp. KNU1 and MIC of AgNPs against *E. coli*, *P. aeruginosa* and *S. aureus* was 6.25, 12.5 and 25 μg/mL whereas, Elbeshehy et al., (2015) synthesized AgNPs using different isolates of *Bacillus* spp., and they found *Bacillus licheniformis* exhibited lowest MIC value when compared to those of *Bacillus pumilus*, *Bacillus persicus* biogenic AgNPs. From the current study AgNPs inhibitory effect was found to be consistent with the studies of Elbeshehy et al., (2015). Biogenic AgNPs were also tested for their *in vitro* anti *H. pylori* activity using three different strains of *H. pylori* and the minimal inhibition concentration shown in Table 2. The MIC results revealed *H. pylori* NCTC 11637 displayed lower activity (24 μg/mL) compared to *H. pylori* J99 (15 μg/mL) and *H. pylori* UM066 (14.5 μg/mL) as shown in Table 1. This agrees well with the disc diffusion assay result. However, increasing the nanoparticle concentration (≤24 μg/mL) inhibits the growth of *H. pylori* NCTC 11637.

3.3.3. Bacteria viability assay

The bacterial viability assay was performed using the bacterial strains of *P. aeruginosa*, *E. coli*, *B. cereus* and *S. aureus* after 30 min exposure with the AgNPs. The bacteria without addition of AgNPs served as the control. Syto 9 is the green fluorescent dye which binds with the viable and healthy bacterial cells, while the PI dye is membrane-impermeable and commonly used to stain cells with damaged or compromised membranes and emits red fluorescence, which usually indicates dead cells (Kang et al., 2007). The control bacteria bind with the live cell binding dye SYTO 9 and visible green fluorescent colour indicating the control cells were healthy and viable (Fig. 4Ai–Di). The four bacterial strains of *E. coli*, *P. aeruginosa*, *S. aureus* and *B. cereus* were mixed with their bactericidal concentration (8, 11.5, 13.5, 14 μg/mL) of AgNPs; after 30 min of incubation, visible fluorescent red colour indicated (Fig. 4Aii–Dii) more than 20% of dead cells (Fig. 4E). Finally, the fluorescent red colour witnessed after 60 min of incubation with AgNPs showed near-complete cell death of bacterial cells (Fig. 4Aiii–Diii). However, almost all the bacterial cells were killed after treatment with nanoparticles, showing significant bactericidal activity (Wu et al., 2010; Gallardo-Moreno et al., 2010). From the observed results it is proposed that AgNPs were effectively inducing membrane damage which leads to leakage of intracellular metabolites through the permeabilized membranes (Humblot et al., 2009).

3.3.4. SEM morphological study

The morphological changes of AgNPs-treated bacteria were extensively studied by SEM. The test bacterial strains of *B. cereus*, *S. aureus*, *E. coli* and *P. aeruginosa* control without nanoparticles treatment showed smooth and damage-free cells (Fig. 5A–D). In the four bacterial strains treated with AgNPs, after 60 min of incubation, dramatic changes were observed in the bacterial morphology. The membrane integrity of AgNPs treated bacterial cells was lost. In the case of *P. aeruginosa* the flagella, which were observed in untreated cells, were completely missing after the AgNPs treatment. After 60 min of incubation almost all the cells showed rumples and had lost their original morphological structure (Fig. 5E–H). The formation of rumples and loss of membrane integrity of AgNPs-treated bacterial cells were similar to the findings of a previous report (Lu et al., 2003).

3.3.5. Release of intracellular protein – FITC

Remarkably, the AgNPs induced bacterial membrane damage and leakage of amino acids from cells, which was confirmed by FITC staining. FITC is widely used in biology and medicine as a fluorescent marker for labelling various proteins. The AgNPs treated bacterial strains of *S. aureus*, *E. coli*, *B. cereus* and *P. aeruginosa* culture supernatant were stained with FITC-I and the green fluorescent spots were observed under CLSM. The green spots observed (Fig. 6E–H) suggested that the aminoacids had leaked out from the bacterial cells following the AgNPs treatment (Li et al., 2013). Green fluorescent spots were not observed in the control sample which indicates healthy and viable bacterial cells (Fig. 6A–D).

3.4. Cytotoxicity effect of AgNPs against HEp-2 cells

Despite its potent antibacterial activity and wide biological applications, the use of AgNPs as therapeutic agent is limited due to their potential for cytotoxic activity against mammalian cells (Mohanty et al., 2012). In this study we tested the cytotoxicity of *P. putida* synthesized AgNPs against HEp-2 cells by the MTT assay, which relies on the fact that metabolically active cells reduce MTT to purple formazan. Hence, the intensity of dye read at 570 nm is directly proportional to the number of viable cells. AgNPs exerted no significant cytotoxic effect at 25 μg/mL concentration (Fig. 7) which was found to be lethal for the bacteria tested in this study, indicating that the biogenic AgNPs are able to display antibacterial activity without being harmful to HEp-2 cells at this concentration. Treatment with increasing dose (50 μg/mL AgNPs) resulted in approximately 20% reduction in cell viability. However, the higher dose 100 μg/mL leads to the cells losing approximately 70% of viability. The IC_{50} value of this assay was calculated at 12.5 μg/mL concentration followed by Lokina et al., (2014). Earlier studies reported that the *in vitro* cytotoxic property of AgNPs synthesized from *Piper longum* plant extract against HEp-2 cancer cell line whereas 49% viability was observed at 31.25 μg/mL concentration of AgNPs (Jacob et al., 2012). It was also reported AgNPs showed dose dependent toxicity to the Hep-2 cells (Satyavani et al., 2011). The specific reason and mechanism for dose-dependent cytotoxicity of AgNPs against HEp-2 cells at high concentrations will need to be established for further study.

4. Conclusions

We summarize, AgNPs were synthesized using culture supernatant of *P. putida* MPV2 derived from silver mining soil. Synthesis and stability characterized HRTEM and spectral analysis showed that bioreduction occurred in both cell membrane and supernatant with good stability up to three months with 6–16 nm size range. SEM analysis revealed the interactions of AgNPs with bacterial membranes by either adhesion and or penetration into the lipid bilayers. Antibacterial effect of

biogenic AgNPs found that upon penetration of cell membrane, AgNPs induce the excretion of intracellular metabolites and lead to the considerable aberration of bacterial cells. Biogenic AgNPs are owing to their low toxicity (25 μg/mL) to human adenocarcinoma HEp-2 cell line. These preliminary antibacterial mechanisms would pave a way to understand the effects on bacterial cells. The results provide critical evidence of AgNPs to achieve designated goals in their antibacterial and therapeutic applications.

Note

16S rRNA sequence of *P. putida* **MPV2** was deposited in GenBank (NCBI) with accession number **JX237836**.

Funding

This research was supported by High Impact Research Chancellory Grant UM.C/625/1/HIR/MoE/CHAN/13/2 (Account No. H-50001-A000032) from the University of Malaya-Ministry of Education, Malaysia.

Acknowledgement

The authors would like to thank Dr. Tarlochan Singh for proofreading this manuscript.

Appendix A. Supplementary material

Supplementary data associated with this article can be found, in the online version, at http://dx.doi.org/10.1016/j.arabjc.2015.11.011.

References

Angajala, G., Ramya, R., Subashini, R., 2014. In-vitro anti-inflammatory and mosquito larvicidal efficacy of nickel nanoparticles phytofabricated from aqueous leaf extracts of *Aegle marmelos* Correa. Acta Tropica 135, 19–26.

Ansari, S.A., Khan, M.M., Ansari, M.O., Lee, J., Cho, M.H., 2014. Visible light-driven photocatalytic and photoelectrochemical studies of Ag–SnO_2 nanocomposites synthesized using an electrochemically active biofilm. RSC Adv. 2014 (4), 26013.

Barwal, I., Ranjan, P., Kateriya, S., Yadav, S.C., 2011. Cellular oxidoreductive proteins of *Chlamydomonas reinhardtii* control the biosynthesis of silver nanoparticles. J. Nanobiotechnol. 9, 56.

Cai, W., Wu, J., Xi, C., Ashe, A.J., Meyerhoff, M.E., 2011. Carboxylebselen-based layer-by-layer films as potential antithrombotic and antimicrobial coatings. Biomaterials 32, 7774–7784.

Chang, C.H., Huang, W.Y., Lai, C.H., Hsu, Y.M., Yao, Y.H., Chen, T.Y., Wu, J.Y., Peng, S.F., Lin, Y.H., 2011. Development of novel nanoparticles shelled with heparin for berberine delivery to treat *Helicobacter pylori*. Acta Biomater. 2, 593–603.

Elbeshehy, E.K.F., Elazzazy, A.M., Aggelis, G., 2015. Silver nanoparticles synthesis mediated by new isolates of *Bacillus* spp., nanoparticle characterization and their activity against Bean Yellow Mosaic Virus and human pathogens. Front Microbiol. 6, 453.

Faria, A.F.D., Martinez, D.S.T., Meira, S.M.M., deMoraes, A.C.M., Brandelli, A., Filho, A.G.S., Alves, O.L., 2014. Anti-adhesion and antibacterial activity of silver nanoparticles supported on graphene oxide sheets. Colloids Surf. B 113, 115–124.

Gajbhiye, M., Kesharwani, J., Ingle, A., Gade, A., Rai, M., 2009. Fungus-mediated synthesis of silver nanoparticles and their activity against pathogenic fungi in combination with fluconazole. Nanotechnol. Biol. Med. 5, 382–386.

Gallardo-Moreno, A.M., Pacha-Olivenza, M.A., Fernández-Calderón, M.C., Pérez-Giraldo, C., Bruquea, J.M., Gonzalez-Martin, M.L., 2010. Bactericidal behaviour of Ti_6Al_4V surfaces after exposure to UV–C light. Biomaterials 31, 5159–5168.

Gopinath, V., MubarakAli, D., Priyadarshini, S., Priyadharsshini, N. M., Thajuddin, N., Velusamy, P., 2012. Biosynthesis of silver nanoparticles from *Tribulus terrestris* and its antimicrobial activity: a novel biological approach. Colloids Surf. B 96, 69–74.

Gopinath, V., Priyadarshini, S., Priyadharshini, N.M., Pandian, K., Velusamy, P., 2013. Biogenic synthesis of antibacterial silver chloride nanoparticles using leaf extracts of *Cissus quadrangularis* Linn. Mater Lett. 91, 224–227.

Gopinath, V., Velusamy, P., 2013. Extracellular biosynthesis of silver nanoparticles using *Bacillus* sp. GP-23 and evaluation of their antifungal activity towards *Fusarium oxysporum*. Spectrochim. Acta A 106, 170–174.

Humblot, V., Yala, J.F., Thebault, P., Boukerma, K., Héquet, A., Berjeaud, J.M., Pradier, C.M., 2009. The antibacterial activity of Magainin I immobilized onto mixed thiols self-assembled monolayers. Biomaterials 30, 3503–3512.

Iwanczak, F., Iwanczak, B., 2012. Treatment of *Helicobacter pylori* infection in the aspect of increasing antibiotic resistance. Adv. Clin. Exp. Med. 21, 671–680.

Jacob, S.J.P., Finub, J.S., Narayanan, A., 2012. Synthesis of silver nanoparticles using *Piper longum* leaf extracts and its cytotoxic activity against Hep-2 cell line. Colloids Surf. B 91, 212–214.

Kalpana, D., Lee, Y.S., 2013. Synthesis and characterization of bactericidal silver nanoparticles using cultural filtrate of simulated microgravity grown *Klebsiella pneumoniae*. Enz. Microb. Technol. 52, 151–156.

Kang, S., Pinault, M., Pfefferle, L.D., Elimelech, M., 2007. Single-walled carbon nanotubes exhibit strong antimicrobial activity. Langmuir 23, 8670–8673.

Khan, M.M., Ansari, S.A., Amal, M.I., Lee, J., Cho, M.H., 2013. Highly visible light active Ag@TiO_2 nanocomposites synthesized using an electrochemically active biofilm: a novel biogenic approach. Nanoscale 5, 4427.

Khan, M.M., Ansari, S.A., Lee, J.H., Ansari, M.O., Lee, J., Cho, M. H., 2014. Electrochemically active biofilm assisted synthesis of Ag@CeO_2 nanocomposites for antimicrobial activity, photocatalysis and photoelectrodes. J. Colloid Interface Sci. 431, 255–263.

Khan, M.M., Kalathil, S., Lee, J., Cho, M.H., 2012. Synthesis of cysteine capped silver nanoparticles by electrochemically active biofilm and their antibacterial activities. Bull. Korean Chem. Soc. 33 (8), 2592–2596.

Li, S., Wang, Z., Wei, Y., Wu, C., Gao, S., Jiang, H., Zhao, X., Yan, H., Wang, X., 2013. Antimicrobial activity of a ferrocene-substituted carborane derivative targeting multidrug-resistant infection. Biomaterials 34, 902–911.

Lokina, S., Stephen, A., Kaviyarasan, V., Arulvasu, C., Narayanan, V., 2014. Cytotoxicity and antimicrobial activities of green synthesized silver nanoparticles. Eur. J. Med. Chem. 76, 256–263.

Lu, Z.X., Zhou, L., Zhang, Z.L., Shi, W.L., Xie, Z.X., Xie, H.Y., Pang, D.W., Shen, P., 2003. Cell damage induced by photocatalysis of TiO_2 thin films. Langmuir 19, 8765–8768.

Madhavan, P., Hong, P.Y., Sougrat, R., Nunes, S.P., 2014. Silver-enhanced block copolymer membranes with biocidal activity. ACS Appl. Mater. Interfaces 6, 18497–18501.

Markowska, K., Grudniak, A.M., Wolska, K.I., 2013. Silver nanoparticles as an alternative strategy against bacterial biofilms. Acta Biochim. Pol. 60, 523–530.

Mohan, S., Oluwafemi, O.S., George, S.C., Jayachandran, V.P., Lewu, F.B., Songca, S.P., Kalarikkal, N., Thomas, S., 2014. Completely green synthesis of dextrose reduced silver nanoparticles, its antimicrobial and sensing properties. Carbohyd. Polym. 106, 469–474.

Mohanty, S., Mishra, S., Jena, P., Jacob, B., Sarkar, B., Sonawane, A., 2012. An investigation on the antibacterial, cytotoxic, and

antibiofilm efficacy of starch-stabilized silver nanoparticles. Nanomed. Nanotechnol. Biol. Med. 8, 916–924.

MubarakAli, D., Arunkumar, J., Nag, H.K., SheikSyedIshack, K.A., Baldev, E., Pandiaraj, D., Thajuddin, N., 2013. Gold nanoparticles from Pro and eukaryotic photosynthetic microorganisms- Comparative studies on synthesis and its application on biolabelling. Colloids Surf. B 103, 166–173.

MubarakAli, D., Arunkumar, J., Pooja, P., Subramanian, G., Thajuddin, N., Harbi, N., 2015a. Synthesis and characterization of biocompatible tenorite nanoparticles for implant coatings with potential property against biofilm formation. Saudi Pharma. J. 23 (4), 421–428.

MubarakAli, D., Sang-Yul, L., Seong-Cheol, K., Jung-Wan, K., 2015b. One-step synthesis and characterization of broad spectrum antimicrobial efficacy of cellulose/silver nanobiocomposites using solution plasma process. RSC Adv. 5, 35052–35060.

MubarakAli, D., Thajuddin, N., Jeganathan, K., Gunasekaran, M., 2011. Plant extract mediated synthesis of silver and gold nanoparticles and its antibacterial activity against clinically isolated pathogens. Colloids Surf. B 85, 360–365.

Mukherjee, P., Roy, M., Mandal, B.P., Dey, G.K., Mukherjee, P.K., Ghatak, J., Tyagi, A.K., Kale, S.P., 2009. Green synthesis of highly stabilized nanocrystalline silver particles by a non-pathogenic and agriculturally important fungus *T. Asperellum*. Nanotechnology 19, 75110.

Muniyappan, N., Nagarajan, N.S., 2014. Green synthesis of silver nanoparticles with *Dalbergia spinosa* leaves and their applications in biological and catalytic activities. Proc. Biochem. 49, 1054–1061.

Pathak, A., Blair, V.L., Ferrero, R.L., Mehring, M., Andrews, P.C., 2014. Bismuth(III) benzohydroxamates: powerful antibacterial activity against *Helicobacter pylori* and hydrolysis to a unique Bi_{34} oxido-cluster $[Bi_{34}O_{22}(BHA)_{22}(H\text{-}BHA)_{14}(DMSO)_6]$. Chem. Commun. 50, 15232–15234.

Priyadarshini, S., Gopinath, V., Priyadharsshini, N.M., Velusamy, P., 2013. Synthesis of anisotropic silver nanoparticles using novel strain, *Bacillus flexus* and its biomedical application. Colloids Surf. B 102, 232–237.

Rai, M., Yadav, A., Gade, A., 2009. Silver nanoparticles as a new generation of antimicrobials. Biotechnol. Adv. 27, 76–83.

Sanghi, R., Verma, P., 2009. Biomimetic synthesis and characterisation of protein capped silver nanoparticles. Biores. Technol. 100, 501–504.

Sastry, M., Ahmad, A., Khan, M.I., Kumar, R., 2003. Biosynthesis of metal nanoparticles using fungi and actinomycete. Curr. Sci. 85, 170.

Satyavani, K., Gurudeeban, S., Ramanathan, T., Balasubramanian, T., 2011. Biomedical potential of silver nanoparticles synthesized from calli cells of *Citrullus colocynthis* (L.) Schrad. J. Nanobiotechnol. 9, 43.

Shao, W., Liu, X., Min, H., Dong, G., Feng, Q., Zuo, S., 2015. Preparation, characterization, and antibacterial activity of silver nanoparticle-decorated graphene oxide nanocomposite. ACS Appl. Mater. Interfaces 7, 6966–6973.

Shivshankar, S., Ahmad, A., Sastry, M., 2003. Geranium leaf assisted biosynthesis of silver nanoparticles. Biotechnol. Prog. 19, 1627–1631.

Tamboli, D.P., Lee, D.S., 2013. Mechanistic antimicrobial approach of extracellularly synthesized silver nanoparticles against gram positive and gram negative bacteria. J. Hazard. Mater. 260, 878–884.

Teh, X., Khosravi, Y., Lee, W.C., Leow, A.H.R., Loke, M.F., Vadivelu, J., Goh, K.L., 2014. Functional and molecular surveillance of *Helicobacter pylori* antibiotic resistance in Kuala Lumpur. PLoS ONE 9, 101481.

Wu, P., Imlay, J.A., Shang, J.K., 2010. Mechanism of *Escherichia coli* inactivation on palladium-modified nitrogen-doped titanium dioxide. Biomaterials 31, 7526–7533.

Xie, J., Lee, J.Y., Wang, D.I., Ting, Y.P., 2007. Silver nanoplates: from biological to biomimetic synthesis. ACS Nano, 429–439.

Yang, C., Jung, S., Yi, H., 2014. A biofabrication approach for controlled synthesis of silver nanoparticles with high catalytic and antibacterial activities. Biochem. Eng. J. 89, 10–20.

Please cite this article in press as: Gopinath, V. et al., Biogenic synthesis, characterization of antibacterial silver nanoparticles and its cell cytotoxicity. Arabian Journal of Chemistry (2015), http://dx.doi.org/10.1016/j.arabjc.2015.11.011